Tissue Eng Regen Med (2019) 16(4):395–403
https://doi.org/10.1007/s13770-019-00195-x

Online ISSN 2212-5469

ORIGINAL ARTICLE

Bone Morphogenetic Protein 2-Conjugated Silica Particles Enhanced Early Osteogenic Differentiation of Adipose Stem Cells on the Polycaprolactone Scaffold

Ki Joo Kim[1] · Moon Seop Choi[1,2] · Jin Hyung Shim[3] · Jong-Won Rhie[1]

Received: 18 March 2019 / Revised: 3 May 2019 / Accepted: 16 May 2019 / Published online: 18 June 2019

Abstract

BACKGROUND: Silica particles (SPs) induce cell proliferation and osteogenic differentiation. We reported that SPs in the scaffold induced early stage osteogenic differentiation.

METHODS: A polycaprolactone (PCL) scaffold was fabricated with a 10 wt% SPs. The surface of PCL scaffold was coated with a 10 μg/mL collagen solution. Next, the scaffold was conjugated with 2 μM SPs, 2 μg/mL bone morphogenetic protein 2 (BMP2), or 2 μM BMP2-conjugated SPs (BCSPs). Green fluorescent protein-coupled BMP2 was applied to fabricate the scaffold. The fluorescence intensity was analyzed by confocal microscopy. The mRNA levels of the early osteogenic differentiation marker, alkaline phosphatase (ALP), were analyzed by real-time quantitative polymerase chain reaction. Levels of BMP2, RUNX2, ERK1/2, and AKT were assessed by western blotting.

RESULTS: ALP mRNA levels were significantly higher in the BCSP-conjugated scaffold than in the other scaffolds. In the early stage of osteogenic differentiation, the protein levels of BMP2, RUNX2, ERK1/2, and AKT in cells were significantly higher in the BCSP-conjugated scaffold than in other scaffolds. Thus, the BCSP composite scaffold induced rapid osteogenic differentiation.

CONCLUSION: These results suggest that BCSP composite can be used to promote early stage osteogenic differentiation and show promise as a material for use in scaffolds for bone regeneration.

Keywords Silica · Bone morphogenetic protein 2 · Scaffold · Adipose stem cell · Osteogenic differentiation

1 Introduction

Silica is a ceramic material that has been used for bone regeneration in the field of tissue engineering. It was recently shown that when incorporated into bone morphogenetic protein 2 (BMP2) and dexamethasone, mesoporous silica particles (SPs) improved the osteogenic differentiation of bone marrow derived stem cells [1]. Silica based materials have high mechanical strength and are suitable for the regeneration of bone tissues [2]. Silicon nitride protects regenerating bone tissues from bacterial infection [3]. Silica based ceramics and biosilicates enhance the formation of bone-like structures [4]. Various biomaterials, including calcium, zinc, and magnesium, have been shown to improve both ERK1/2 gene expression

Ki Joo Kim and Moon Seop Choi have contributed equally to this work.

Electronic supplementary material The online version of this article (https://doi.org/10.1007/s13770-019-00195-x) contains supplementary material, which is available to authorized users.

✉ Jong-Won Rhie
rhie@catholic.ac.kr

[1] Department of Plastic and Reconstructive Surgery, College of Medicine, The Catholic University of Korea, 222, Banpo-dearo, Seocho-gu, Seoul 06591, Republic of Korea

[2] Grace Plastic Surgery Clinic, 623, KangNam-dearo, Seoul 06524, Republic of Korea

[3] Department of Mechanical Engineering, Korea Polytechnic University, 237, Sangidaehak-ro, Siheung-si, Gyenggi-do 15073, Republic of Korea

and biological action in cell attachment and proliferation [5, 6]. Silicon also induces the proliferation and osteogenesis of osteoblast-like cells [7].

BMP2, like other bone morphogenetic proteins, is an osteoinductive protein [8]. It plays an important role in the development of bone and is involved in the transforming growth factor (TGF)-β signaling pathway and cytokine–cytokine receptor interactions. BMP2 has also been shown to induce osteogenesis in a variety of cell types. Recent studies have demonstrated the use of BMP2 with stem cells to treat bone defects and induce formation of new bone *in vivo* [9].

Runt-related transcription factor 2 (Runx2) is a key transcription factor associated with osteoblast differentiation [10]. Runx2 is activated via the BMP2, ERK, and p38 signaling pathways [11]. Many studies have reported that Runx2 is an essential protein for osteogenic differentiation, particularly osteogenesis in mesenchymal stem cells [12, 13].

Polycaprolactone (PCL) is a bioresorbable material that has previously been used in medicine [14]. Synthetic scaffolds prepared with a variety of materials have been shown to be biocompatible and biodegradable, and have been used as barrier membranes [15, 16]. They have also been used in prototyping systems, such as fused filament fabrication three-dimensional (3D) printers. For example, scaffolds made of biopolymers, including PCL, poly(lactic-co-glycolic acid) (PLGA), and tricalcium phosphate, prepared using 3D printing technology, improved bone formation and treated bone defects in animal models [17].

Adipose stem cells (ASCs) have been used for clinical applications because of their abundance and ease of separation compared with bone marrow stem cells [18]. ASCs have also been used to induce osteogenic differentiation and in cell therapy [19, 20]. ASCs combined with a hydroxyapatite bioceramic scaffold can construct vascularized tissue-engineered bone [20]. Therefore, we used ASCs in this experiment.

In this study, 3D-printed biopolymer/ceramic compositional scaffolds conjugated with SPs, BMP2, or BMP2-conjugated SPs (BCSPs) were evaluated in terms of their ability to induce early stage osteogenic differentiation. The BCSP-conjugated scaffold promoted the initial osteogenic differentiation of ASCs to a greater degree than did the other scaffolds.

2 Materials and methods

2.1 ASC isolation, culture and differentiation

Human ASCs were isolated and cultured as described previously [21]. Cells were obtained from patients in accordance with the guidelines of the institutional review board of Seoul St. Mary's Hospital, Republic of Korea (IRB no. KC17TESI0546). The raw lipoaspirates obtained from patients washed thoroughly with sterile phosphate-buffered saline (PBS; Life Technologies, Carlsbad, CA, USA), minced, and digested with 0.1% type I collagenase (Sigma-Aldrich, St. Louis, MO, USA) in PBS for 30 min at 37 °C in a 5% CO_2 atmosphere with gentle agitation. The collagenase was then inactivated with an equal volume of Dulbecco's modified Eagle's medium (DMEM; Life Technologies, Carlsbad, CA, 94 USA) containing 10% fetal bovine serum (FBS; Wisent Inc., St. Bruno, Quebec, Canada) and 1% antibiotic/antimycotic (Life Technologies). The cells were harvested by centrifugation at 250 × *g* for 5 min and filtered through a 100 μm mesh to remove debris. Cells were plated onto conventional culture plates in DMEM containing 10% FBS and 1% antibiotic/antimycotic at 37 °C in a humidified atmosphere with 5% CO_2. The culture medium was changed every 3 days. ASCs were cultured until passage 3, and subsequently cultured on the scaffolds at 1×10^5 cells/scaffold for 7 days. The proliferation medium was replaced with osteogenic differentiation medium, which was replenished every 3 days. The composition of the osteogenic differentiation medium was as follows: 0.1 μM dexamethasone (Sigma-Aldrich, St. Louis, MO, USA), 10 mM glycerol phosphate (Sigma-Aldrich, St. Louis, MO, USA), and 35.7 μg/mL ascorbic acid-phosphate (Sigma-Aldrich, St. Louis, MO, USA) in 100 mL of DMEM containing 10% FBS and 1% antibiotic/antimycotic.

2.2 Preparation of SPs and BCSPs

SPs were prepared as described previously [21]. Silica gel was prepared by a chemical neutralization reaction, in which hydrochloric acid was mixed with a solution of reagent-grade sodium silicate (SiO_2 26.5%, Na_2O 10.6%, and H_2O 62.9%; Sigma-Aldrich, St. Louis, MO, USA); 5 g of SPs were synthesized from 20 g of sodium silicate solution according to the law of conservation of mass. BMP2-conjugated silica particles (BCSPs) were prepared by suspending 5 g of SPs in a 50 μg/mL BMP2 solution for 24 h at 4 °C. Green fluorescent protein (GFP)-conjugated BMP2 protein was applied to fabricate the scaffold. The surface of the SPs and BCSPs was observed using a transmission electron microscope (TEM; JEM1010, Jeol, Tokyo, Japan) after negative staining according to Brenner's method [22]. The fluorescence of GFP on the surface of the BCSPs was visualized by confocal microscopy (LSM 510 Meta, Zeiss, Oberkochen, Germany).

2.3 Scaffold fabrication

Polycaprolactone (PCL; Mw 45,000; Sigma-Aldrich, St. Louis, MO, USA) containing SPs (10 wt%) was used to

fabricate scaffolds by 3D printing using Shim's method with two dispensing heads of a multi-head deposition system (MHDS) [17]. The fabricated scaffolds were submerged in a 10 μg/mL collagen solution for 24 h at 4 °C to allow coating of the surface. Next, 2 μM SPs, 2 μg/mL BMP2, or 2 μM BCSPs-conjugated to the surface of the collagen-coated scaffolds for 24 h at 4 °C (Fig. 1A). Finally, the scaffolds were washed twice with phosphate-buffered saline (PBS). The surface of the scaffolds was observed by confocal microscopy (LSM 510 Meta, Zeiss, Oberkochen, Germany) and scanning electron microscope (SEM; S2460 N, Hitachi Ltd, Tokyo, Japan) (Fig. 1B–E).

2.4 Analysis of mRNA levels by qRT-PCR

Total RNA was extracted from ASCs in the scaffolds using TRIzol reagent (Invitrogen, Carlsbad, CA, USA) according to the manufacturer's instructions. The purity of the extracted RNA was then calculated (ND-1000, Thermo Scientific, Waltham, MA, USA). The cDNA was prepared by reverse transcription of 1 mg total RNA from each sample using M-MLV Reverse Transcriptase (Invitrogen, Carlsbad, CA, USA). Quantitative real-time polymerase chain reaction (qRT-PCR) was performed using a Power SYBR mixture with 0.5 μL each of the forward and reverse primers, 25 μL of Power SYBR Green PCR Master Mix (Applied Biosystems Inc., Carlsbad, CA, USA), and 1 μL of sample on an ABI Prism 7900 HT instrument (Applied Biosystems Inc., Carlsbad, CA, USA). qRT-PCR was performed under the following conditions: denaturation for 2 min at 50 °C, annealing for 10 min at 95 °C, and extension (40 cycles) for 15 s at 95 °C and 1 min at 60 °C. Human sequence-specific oligonucleotide primers designed based on published sequences were as follows: ALP forward, 5′-ATG TCA TCA TGT TCC TGG GAG AT-3′ and reverse, 5′-TGG AGC TGA TCC TTG AGG-3′.

2.5 Analysis of protein levels by western blotting

Cultured ASCs in the scaffold were washed twice with cold-PBS, and 100 μL of T-PER Protein Extraction Reagent (Thermo Fisher Scientific, Rockford, IL, USA) was added to the culture dish. After scraping, the contents of the dish were transferred into a 1.5 mL tube and shaken at 4 °C for 1 min. The samples were centrifuged at 11,000 × *g* for 15 min at 4 °C. The supernatant was transferred into a 1.5 mL flash tube. Quantitative analysis was performed using the Bradford assay (Bio-Rad, Hercules, CA, USA). For western blot analysis, equal amounts of protein (15 μg) were electrophoresed on 10% sodium dodecyl sulfate polyacrylamide gels. After electrophoresis, proteins were transferred from the gel onto a 0.45 μm nitrocellulose transfer membrane (Whatman GmbH, Dassel, Germany) using an electrical transfer system. Non-specific binding was blocked by incubation with 5% skim milk (BD Biosciences, Franklin Lakes, NJ, USA) in TBST buffer (5 mM Tris–HCl, pH 7.6, 136 mM NaCl, and 0.1% Tween 20) for 1 h. The blots were then incubated with the appropriate primary antibody (dilution: 1:2000) for 24 h at 4 °C, after which they were washed thrice with 1 × TBST. Next, the blots were incubated for 2 h at 26 °C with a secondary antibody (dilution: 1:5000). The blots were washed thrice with 1 × TBST and developed using enhanced chemiluminescence western detection reagents (GE Healthcare, Buckinghamshire, UK). The blots were then analyzed using a luminescent image analysis instrument (Fuji Photofilm, Tokyo, Japan). The Multi-Gauge program (ver. 3.0) was used for quantitative assays. The primary antibodies used were specific for BMP2 (Santa Cruz Biotechnology, Dallas, TX, USA), RUNX2 (Santa Cruz Biotechnology, Dallas, TX, USA), ERK1/2 (Cell Signaling Technology Inc., Danvers, MA, USA), *p*-ERK1/2 (Cell Signaling Technology Inc., Danvers, MA, USA), AKT (Cell Signaling Technology Inc., Danvers, MA, USA), *p*-AKT (Cell Signaling Technology Inc., Danvers, MA, USA), and actin (Sigma-Aldrich, St. Louis, MO, USA). The secondary antibodies used were anti-rabbit IgG-horse radish peroxidase (HRP) (Santa Cruz Biotechnology, Dallas, TX, USA) and anti-mouse IgG-HRP conjugate (Santa Cruz Biotechnology, Dallas, TX, USA).

2.6 Statistical analysis

All values are presented as mean ± standard deviation (SD). Analysis was performed using IBM Statistics 24 (SPSS Inc., New York. NY, USA). The Kruskal–Wallis test was performed to determine the significance of all data. $*P < 0.05$ was considered statistically significant.

3 Results

3.1 Analysis of SPs and BCSPs

The presence of SPs and BCSPs was confirmed using a TEM and a confocal microscope. The TEM image showed SPs as black particles (Fig. 2A, B) and BCSPs as shadow particles after negative staining (Fig. 2C, D). The same particles were also observed using confocal microscopy. The surface of the BCSPs showed a strong green fluorescence signal (Fig. 2E–G); in contrast, no green fluorescence signal was observed on the surface of the SPs.

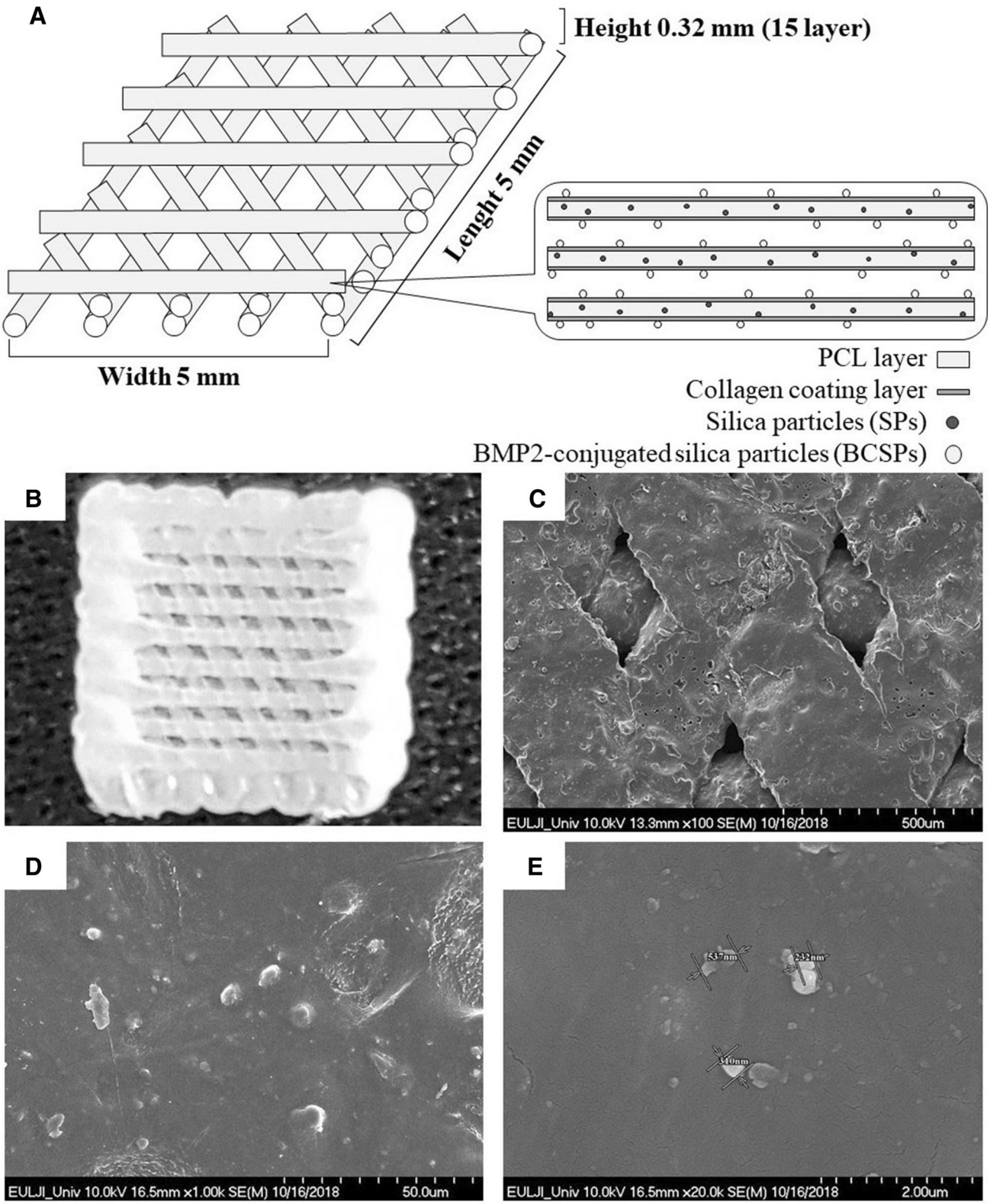

Fig. 1 Preparation of a polycaprolactone/silica particle (PCL/SP) scaffold with bone morphogenetic protein 2 (BMP2)-conjugated SPs (BCSPs) by 3D printing. PCL scaffolds was fabricated with 10 wt% SPs. The prepared scaffold was coated with a 10 μg/mL collagen solution and its surface was conjugated with 2 μM BCSPs. **A** Structure of the fabricated scaffold. **B** Image of fabricated scaffold by 3D printing. **C–E** SEM images of the BCSP-conjugated scaffold

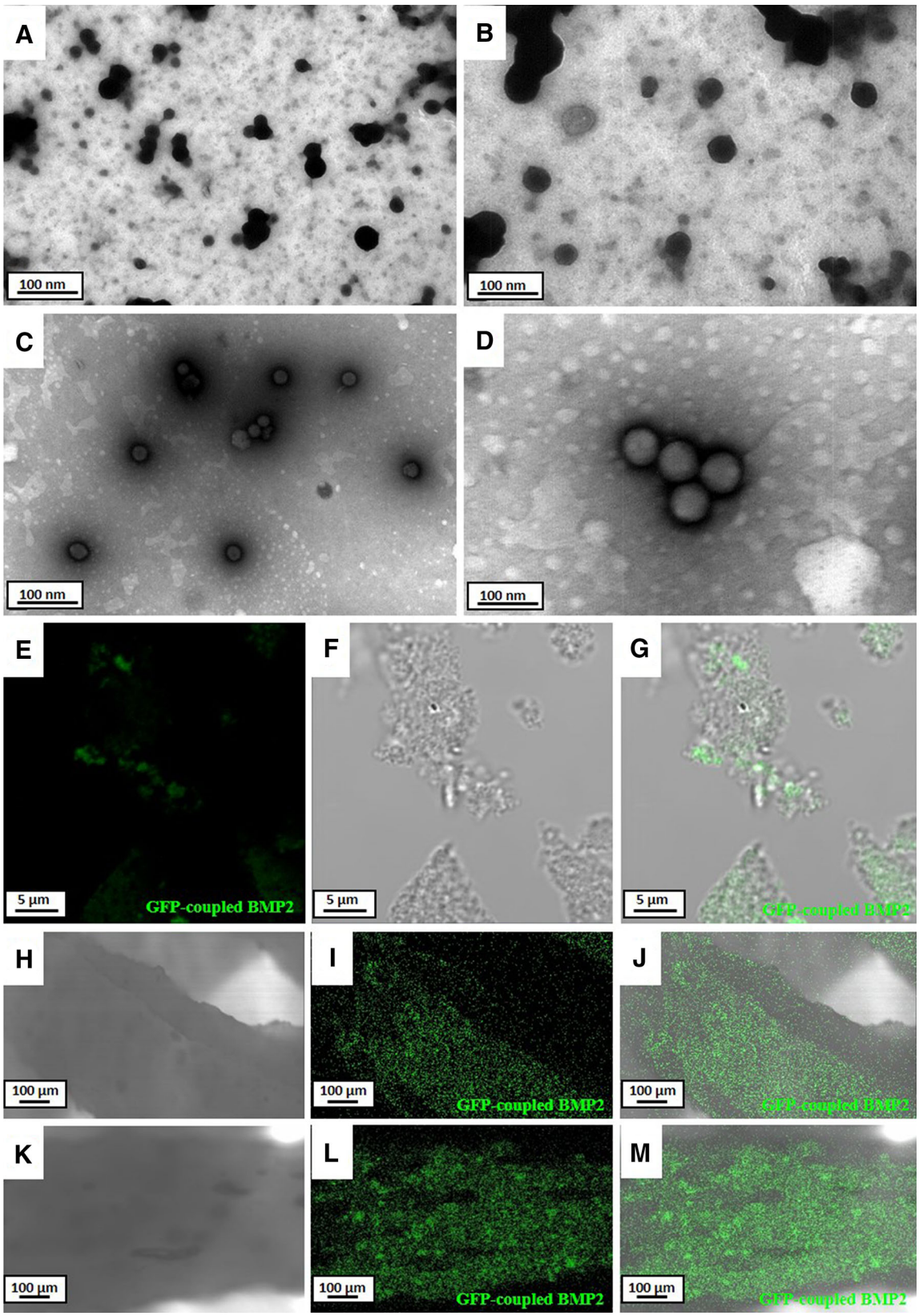
A
100 nm
B
100 nm
C
100 nm
D
100 nm
E
5 μm
GFP-coupled BMP2
F
5 μm
G
5 μm
GFP-coupled BMP2
H
100 μm
I
100 μm
GFP-coupled BMP2
J
100 μm
GFP-coupled BMP2
K
100 μm
L
100 μm
GFP-coupled BMP2
M
100 μm
GFP-coupled BMP2

◀**Fig. 2** Transmission electron microscopy (TEM) and confocal microscopy analysis of prepared SP, BCSP, and (BMP2 or BCSP)-conjugated scaffolds. Green fluorescence indicates the presence of green fluorescence protein (GFP) fused with BMP2 protein. **A**, **B** SP appear black after negative staining by TEM. **C**, **D** BCSP appear as shadows after negative staining by TEM. Shadows indicate that BMP2 was uniformly conjugated on the surface of the SP. **E–G** GFP-conjugated BMP2 on the surface of the BCSPs by confocal microscopy. **H–J** Surface of the BMP2-conjugated scaffold by confocal microscopy. **K–M** Surface of the BCSP-conjugated scaffold by conforcal microscopy

3.2 Analysis of scaffolds

The scaffolds were prepared after soaking in a 10 μg/mL collagen solution. And, their surface was conjugated with SPs, BMP2, or BCSPs. The surface of the BMP2-conjugated scaffold exhibited uniform expression of GFP (Fig. 2H–J). Similarly, the surface of the BCSP-conjugated scaffold also showed expression of GFP (Fig. 2K–M).

3.3 Analysis of mRNA level

We assessed the ability of the SP-conjugated, BMP2-conjugated, and BCSP-conjugated scaffolds to induce early osteogenic differentiation of ASCs by measuring ALP mRNA levels using qRT-PCR. The ALP mRNA levels of cells were higher in the SP-conjugated scaffold than in the non-conjugated scaffold. The ALP mRNA levels of cells were significantly higher in the BCSP-conjugated scaffold than in the BMP2-conjugated scaffold. Furthermore, ALP mRNA levels were significantly higher in cells in the BCSP-conjugated scaffold than in those in the SP-conjugated scaffold (Fig. 3) ($p < 0.05$).

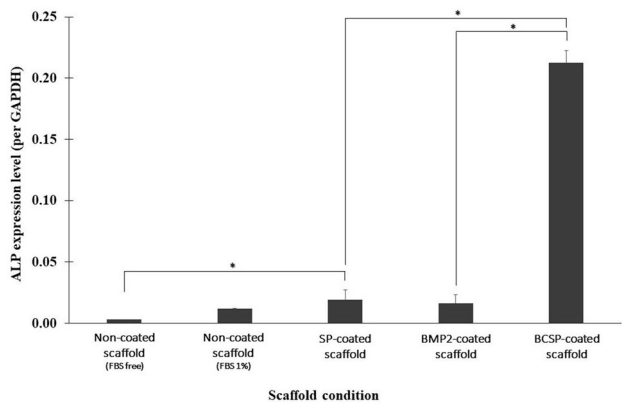

Fig. 3 Alkaline phosphatase (ALP) mRNA levels in adipose stem cells (ASCs) cultured on scaffolds conjugated with SP, BMP2, or BCSP as determined by real-time polymerase chain reaction. The BCSP-conjugated scaffold shows significantly higher ALP mRNA levels compared to the SP-conjugated scaffold (*$p < 0.05$)

3.4 Analysis of protein levels

We next assessed the effects of the SP-conjugated, BMP2-conjugated, and BCSP-conjugated scaffolds on the levels of BMP2, RUNX2, ERK1/2, and AKT (Fig. 4A). BMP2 levels were significantly higher in the BCSP-conjugated scaffold relative to the other scaffolds (Fig. 4B). RUNX2 levels were highest in the BMP2-conjugated scaffold and were significantly higher in the BCSP-conjugated scaffold than in the SP-conjugated scaffold (Fig. 4C) (***$p < 0.001$). Furthermore, ERK1/2 levels were significantly higher in the BCSP-conjugated scaffold relative to the other scaffolds (Fig. 4D) (**$p < 0.001$). AKT, a marker of cell survival, did not differ among the scaffolds (Fig. 4E) (*$p < 0.05$).

4 Discussion

We report here that SP-conjugated, BMP2-conjugated, and BCSP-conjugated functional PCL scaffolds induced early stage osteogenic differentiation. Many studies have shown that PCL based scaffolds induce osteogenic differentiation of cells. Yao et al. [23] reported that a PCL/poly lactic acid (PLA) nanofibrous scaffold strongly induced osteogenesis for cranial bone formation. Biodegradable extracellular matrix (ECM)-coated PCL microcarriers induced differentiation of human bone marrow stromal cells during bone formation [24]. Shim et al. [25] showed that PCL/PLGA/collagen-mixed scaffolds promoted proliferation and osteogenic differentiation of adipose stem cells. We fabricated functional scaffold with SPs, BMP2, and BCSPs and observated by SEM (Fig. 1).

Three-dimensional scaffolds made of PCL exhibit enhanced porosity compared with two-dimensional scaffolds. Additionally, the properties of 3D scaffolds can be altered by changing the fabrication and pattern-forming methods [26]. 3D scaffolds have also been shown to promote cell attachment, cell proliferation, and the production of new ECM in functional tissue. Moreover, 3D printed scaffolds exhibit better cell affinity [26, 27]. It has been shown that silica based scaffolds induce cell attachment and have high biocompatibility [28]. Nanostructured silicon enhances protein adsorption on cells [29]. A previous study reported that SPs combined with a PLGA scaffold induced proliferation and osteogenic differentiation of ASCs, and increased their proliferation via the ERK1/2 signaling pathway [21]. ERK1/2 signaling is involved in osteogenic differentiation during early differentiation. In addition, ERK1/2 signaling is activated during cell proliferation, differentiation, and migration. The magnitude of these various effects differs depending on the environment surrounding the cells [30]. Thus, activation of ERK1/2

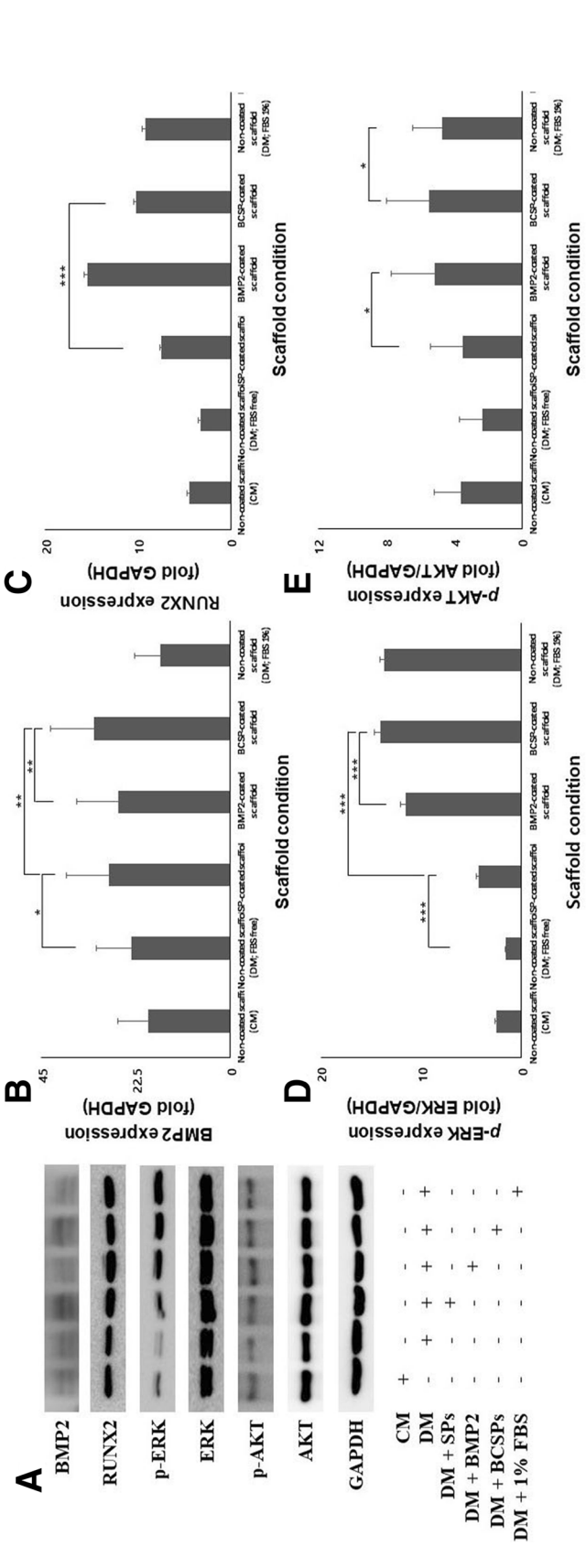

Fig. 4 BMP2, RUNX2, phosphorylated ERK1/2, and phosphorylated AKT levels as determined by western blotting. **A** Western blot analysis results. **B** BMP2, an osteogenic differentiation marker, was significantly expressed in the BCSP-conjugated scaffold relative to the SP-conjugated and BMP2-conjugated scaffolds ($^{*}p < 0.05$, $^{**}p < 0.01$, and $^{***}p < 0.001$). **C** RUNX2 expression was highest in the BMP2-conjugated scaffold. And, the BCSP-conjugated scaffold showed significantly higher expression of RUNX2 compared to the SP-conjugated scaffold ($^{***}p < 0.001$). **D** ERK1/2 was significantly expressed in the BCSP-conjugated scaffold compared to the SP-conjugated and BMP2-conjugated scaffolds ($^{***}p < 0.001$). **E** AKT, a marker of cell survival, did not differ among the scaffolds ($^{*}p < 0.05$)

signaling in osteogenic differentiation can lead to early stage osteogenic differentiation.

Transmission electron microscopy (TEM) is a microscopy technique in which a beam of electrons is transmitted through a specimen to form an image. Negative staining is an established method for distinguishing between organic and inorganic materials; non-biological or inorganic substances appear black while organic or biological materials are seen as shadows [22]. SPs and BCSPs were visualized by TEM with negative staining. The black stain observed on the surface of the SPs was the inorganic silica ceramic (Fig. 2A, B), and the shadow stain was the organic BMP2 on the surface of BCSPs (Fig. 2C, D). These results indicate that BMP2 was uniformly distributed across the surface of the BCSPs. Additionally, green fluorescence was observed on the surface of the BCSPs (Fig. 2E–G). Thus, the BMP2 coating on the surface of the BCSPs promoted early osteogenic differentiation of ASCs.

BCSPs, which comprise SPs-conjugated with GFP-conjugated BMP2, were observed on the scaffold surface as green fluorescence using confocal microscopy (Fig. 2H–J). This explains why the BMP2-conjugated scaffold also emitted green fluorescence (Fig. 2K–M). The BCSP-conjugated scaffold induced earlier osteogenic differentiation compared to the non-conjugated scaffold. All scaffolds had uniformly distributed particles on their surface. The binding of collagen and BMP2 was likely mediated by the hydroxyl groups on the surface of the SPs. According to the chemical structure of the hydroxyl group of SPs, collagen combines easily with the hydroxyl group of SPs on the surface of the scaffold. This structural feature makes it possible for BCSPs to combine SPs with BMP2 protein (Fig. S1); indeed, most proteins are capable of binding to hydroxyl groups. Two prior studies have used silica and collagen coatings to increase adhesion by cells [31, 32].

ALP is a marker of the early stage of osteogenic differentiation [33]. Estimated ALP mRNA levels have been used to confirm the occurrence of osteogenic differentiation. When the ALP mRNA levels of ASCs cultured in the SP-conjugated, BMP2-conjugated, and BCSP-conjugated scaffolds were evaluated, cells in the BCSP-conjugated scaffold showed significantly higher ALP mRNA levels than those in the other conjugated scaffolds (Fig. 3). Thus, the BCSP-conjugated scaffold had the ability to accelerate the osteogenic differentiation of ASCs. Evaluation of the expression of other signaling pathway factors (Fig. 4A) in the scaffolds revealed that BMP2 and RUNX2 expression levels were higher in the BCSP-conjugated scaffold than in the non-conjugated and SP-conjugated scaffolds (Fig. 4B, C) [34]. Interestingly, RUNX2 expression levels were highest in the BMP2-conjugated scaffold. RUNX2 gene is a master transcription factor to osteogenic differentiation and its activation is necessary BMP2 signaling [35]. BMP2 upregulates RUNX2 signaling that is a key regulator of osteogenic differentiation [36]. Our results showed that BMP2-conjugated scaffold have a lot of activation BMP2-RUNX2 signaling pathway compared to BCSP-conjugated scaffold because BCSP-conjugated scaffold concerned both BMP2 effect and SPs effect. SPs make an impact on mineralization of cells through a MAPK signaling pathway [21]. Phosphorylation of ERK1/2 increases during osteogenic differentiation. ERK1/2 is generally known to concern to osteogenic differentiation through a mitogen-activated protein kinase (MAPK) signaling pathway. Phosphorylation of ERK1/2 was significantly increased in the BCSP-conjugated scaffold compared to the other conjugated scaffolds (Fig. 4D). The greater activation of ERK1/2 in the BCSP-conjugated scaffold implies that induction of early stage osteogenic differentiation by BCSPs was greater than that by SPs or BMP2. Also, AKT is known that is usually regulated to cell survival. Phosphorylation of AKT was observed in the all groups. This result showed that cells are well survived in all groups (Fig. 4E).

Therefore, the BCSP-conjugated scaffold induced early osteogenic differentiation of ASCs more rapidly than did the SP-conjugated or BMP2-conjugated scaffolds. BCSP-conjugated scaffolds could be applied for bone regeneration in the field of tissue engineering.

Acknowledgements This work was financially supported by the Basic Science Research Program through the National Research Foundation of Korea (NRF) funded by the Ministry of Education (2017R1A6A3A11030383 and 2017M3A9E2060428).

Compliance with ethical standards

Conflict of interest All authors declare that they have no conflict of interest.

Ethical statement The study protocol was approved by the institutional review board of Seoul St. Mary's Hospital, Republic of Korea (IRB No. KC17TESI0546).

References

1. Zhou X, Feng W, Qiu K, Chen L, Wang W, Nie W, et al. BMP-2 derived peptide and dexamethasone incorporated mesoporous silica nanoparticles for enhanced osteogenic differentiation of bone mesenchymal stem cells. ACS Appl Mater Interfaces. 2015;7:15777–89.
2. Yang XB, Webb D, Blaker J, Boccaccini AR, Maquet V, Cooper C, et al. Evaluation of human bone marrow stromal cell growth on biodegradable polymer/bioglass composites. Biochem Biophys Res Commun. 2006;342:1098–107.
3. Webster TJ, Patel AA, Rahaman MN, Sonny Bal B. Anti-infective and osteointegration properties of silicon nitride, poly(ether ether ketone), and titanium implants. Acta Biomater. 2012;8:4447–54.

4. Wu C, Chang J, Wang J, Ni S, Zhai W. Preparation and characteristics of a calcium magnesium silicate (bredigite) bioactive ceramic. Biomaterials. 2005;26:2925–31.
5. Shie MY, Chang HC, Ding SJ. Effects of altering the Si/Ca molar ratio of a calcium silicate cement on in vitro cell attachment. Int Endod J. 2012;45:337–45.
6. Zhou H, Wei J, Wu X, Shi J, Liu C, Jia J, et al. The bio-functional role of calcium in mesoporous silica xerogels on the responses of osteoblasts in vitro. J Mater Sci Mater Med. 2010;21:2175–85.
7. Wiens M, Wang X, Schlossmacher U, Lieberwirth I, Glasser G, Ushijima H, et al. Osteogenic potential of biosilica on human osteoblast-like (SaOS-2) cells. Calcif Tissue Int. 2010;87:513–24.
8. Huang H, Dou L, Song J, Luo J. CBFA2T2 is required for BMP-2-induced osteogenic differentiation of mesenchymal stem cells. Biochem Biophys Res Commun. 2018;496:1095–101.
9. Zhang W, Zhu C, Wu Y, Ye D, Wang S, Zou D, et al. VEGF and BMP-2 promote bone regeneration by facilitating bone marrow stem cell homing and differentiation. Eur Cell Mater. 2014;27:1–11.
10. Li Z, Wang W, Xu H, Ning Y, Fang W, Liao W, et al. Effects of altered CXCL12/CXCR10 axis on BMP2/Smad/Runx2/Osterix axis and osteogenic gene expressions during osteogenic differentiation of MSCs. Am J Transl Res. 2017;9:1680–93.
11. Huang RL, Yuan Y, Tu J, Zou GM, Li Q. Opposing TNF-alpha/IL-1beta- and BMP-2-activated MAPK signaling pathways converge on Runx2 to regulate BMP-2-induced osteoblastic differentiation. Cell Death Dis. 2014;5:e1187.
12. Pino AM, Rosen CJ, Rodriguez JP. In osteoporosis, differentiation of mesenchymal stem cells (MSCs) improves bone marrow adipogenesis. Biol Res. 2012;45:279–87.
13. van Zoelen EJ, Duarte I, Hendriks JM, van der Woning SP. TGF β-induced switch from adipogenic to osteogenic differentiation of human mesenchymal stem cells: identification of drug targets for prevention of fat cell differentiation. Stem Cell Res Ther. 2016;7:123.
14. Andalib MN, Lee JS, Ha L, Dzenis Y, Lim JY. Focal adhesion kinase regulation in stem cell alignment and spreading on nanofibers. Biochem Biophys Res Commun. 2016;473:920–5.
15. Koupaei N, Karkhaneh A. Porous crosslinked polycaprolactone hydroxyapatite networks for bone tissue engineering. Tissue Eng Regen Med. 2016;13:251–60.
16. Hua N, Ti VL, Xu Y. Biodegradable effect of PLGA membrane in alveolar bone regeneration on beagle dog. Cell Biochem Biophys. 2014;70:1051–5.
17. Shim JH, Moon TS, Yun MJ, Jeon YC, Jeong CM, Cho DW, et al. Stimulation of healing within a rabbit calvarial defect by a PCL/PLGA scaffold blended with TCP using solid freeform fabrication technology. J Mater Sci Mater Med. 2012;23:2993–3002.
18. Kim CM, Oh JH, Jeon YR, Kang EH, Lew DH. Effects of human adipose-derived stem cells on the survival of rabbit ear composite grafts. Arch Plast Surg. 2017;44:370–7.
19. Castro-Govea Y, Vela-Martinez A, Treviño-Garcia LA. Volumetric lipoinjection of the fronto-orbital and temporal complex with adipose stem cells for the aesthetic restoration of sequelae of craniosynostosis. Arch Plast Surg. 2018;45:128–34.
20. Xia L, Lin K, Jiang X, Fang B, Xu Y, Liu J, et al. Effect of nano-structured bioceramic surface on osteogenic differentiation of adipose derived stem cells. Biomaterials. 2014;35:8514–27.
21. Kim KJ, Joe YA, Kim MK, Lee SJ, Ryu YH, Cho DW, et al. Silica nanoparticles increase human adipose tissue-derived stem cell proliferation through ERK1/2 activation. Int J Nanomedicine. 2015;10:2261–72.
22. Hayer-Hartl M, Bracher A, Hartl FU. The GroEL–GroES chaperonin machine: a nano-cage for protein folding. Trends Biochem Sci. 2016;41:62–76.
23. Yao Q, Cosme JG, Xu T, Miszuk JM, Picciani PH, Fong H, et al. Three dimensional electrospun PCL/PLA blend nanofibrous scaffolds with significantly improved stem cells osteogenic differentiation and cranial bone formation. Biomaterials. 2017;115:115–27.
24. Shekaran A, Lam A, Sim E, Jialing L, Jian L, Wen JT, et al. Biodegradable ECM-coated PCL microcarriers support scalable human early MSC expansion and in vivo bone formation. Cytotherapy. 2016;18:1332–44.
25. Shim JH, Kim AJ, Park JY, Yi N, Kang I, Park J, et al. Effect of solid freeform fabrication-based polycaprolactone/poly(lactic-co-glycolic acid)/collagen scaffolds on cellular activities of human adipose-derived stem cells and rat primary hepatocytes. J Mater Sci Mater Med. 2013;24:1053–65.
26. Hejazi F, Mirzadeh H. Novel 3D scaffold with enhanced physical and cell response properties for bone tissue regeneration, fabricated by patterned electrospinning/electrospraying. J Mater Sci Mater Med. 2016;27:143.
27. Markovic M, Van Hoorick J, Hölzl K, Tromayer M, Gruber P, Nürnberger S, et al. Hybrid tissue engineering scaffolds by combination of three-dimensional printing and cell photoencapsulation. J Nanotechnol Eng Med. 2015;6:0210011–7.
28. Thanyaphoo S, Kaewsrichan J. Synthesis and evaluation of novel glass ceramics as drug delivery systems in osteomyelitis. J Pharm Sci. 2012;101:2870–82.
29. Sommerfeld J, Richter J, Niepelt R, Kosan S, Keller TF, Jandt KD, et al. Protein adsorption on nano-scaled, rippled TiO_2 and Si surfaces. Biointerphases. 2012;7:55.
30. Sun Y, Liu WZ, Liu T, Feng X, Yang N, Zhou HF. Signaling pathway of MAPK/ERK in cell proliferation, differentiation, migration, senescence and apoptosis. J Recept Signal Transduct Res. 2015;35:600–4.
31. Ehlert N, Hoffmann A, Luessenhop T, Gross G, Mueller PP, Stieve M, et al. Amino-modified silica surfaces efficiently immobilize bone morphogenetic protein 2 (BMP2) for medical purposes. Acta Biomater. 2011;7:1772–9.
32. Heinemann S, Coradin T, Worch H, Wiesmann HP, Hanke T. Possibilities and limitations of preparing silica/collagen/hydroxyapatite composite xerogels as load-bearing biomaterials. Compos Sci Technol. 2011;71:1873–80.
33. Xiao HT, Wang L, Yu B. Superparamagnetic iron oxide promotes osteogenic differentiation of rat adipose-derived stem cells. Int J Clin Exp Med. 2015;8:698–705.
34. Samuel S, Ahmad RE, Ramasamy TS, Karunanithi P, Naveen SV, Murali MR, et al. Platelet-rich concentrate in serum free medium enhances osteogenic differentiation of bone marrow-derived human mesenchymal stromal cells. PeerJ. 2016;4:e2347.
35. Chen G, Deng C, Li YP. TGF-β and BMP signaling in osteoblast differentiation and bone formation. Int J Biol Sci. 2012;8:272–88.
36. Lee SY, Koak JY, Kim SK, Heo SJ. Cellular response of anodized titanium surface by poly(lactide-co-glycolide)/bone morphogenic protein-2. Tissue Eng Regen Med. 2018;15:591–9.